BJR

https://doi.org/10.1259/bjr.20180713

Received: 13 August 2018 | Revised: 19 November 2018 | Accepted: 10 December 2018

Cite this article as:
Vanhove C, Goethals I. Magnetic resonance imaging-guided radiation therapy using animal models of glioblastoma. *Br J Radiol* 2019; **92**: 20180713.

SMALL ANIMAL IGRT SPECIAL FEATURE: REVIEW ARTICLE

Magnetic resonance imaging-guided radiation therapy using animal models of glioblastoma

[1]CHRISTIAN VANHOVE, PhD and [2]INGEBORG GOETHALS, MD, PhD

[1]Department of Electronics and Information Systems, Institute Biomedical Technology (IBiTech), Ghent University, Ghent, Belgium
[2]Department of Nuclear Medicine, Ghent University Hospital, Ghent, Belgium

Address correspondence to: Prof Christian Vanhove
E-mail: *Christian.Vanhove@UGent.be*

ABSTRACT

Glioblastoma is the most aggressive and most common malignant primary brain tumour in adults and has a high mortality and morbidity. Because local tumour control in glioblastoma patients is still elusive in the majority of patients, there is an urgent need for alternative treatment strategies. However, to implement changes to the existing clinical standard of care, research must be conducted to develop alternative treatment strategies. A novel approach in radiotherapy is the introduction of pre-clinical precision image-guided radiation research platforms. The aim of this review is to give a brief overview of the efforts that have been made in the field of radiation research using animal models of glioblastoma. Because MRI has become the reference imaging technique for treatment planning and assessment of therapeutic responses in glioblastoma patients, we will focus in this review on small animal radiotherapy combined with MRI.

INTRODUCTION

Glioblastoma (GB) is the most aggressive and most common malignant primary brain tumour in adults and has a high mortality and morbidity.[1] For newly diagnosed patients with a good performance status, the standard of care includes surgery followed by combined external beam radiation therapy (RT) and temozolomide (TMZ), followed by maintenance TMZ. The goal of surgery is to provide maximal tumour resection, with preservation or restoration of neurologic function. Studies have shown that gross total resection enhances overall survival in GB. When maximal surgical resection is not possible, subtotal resection still provides additional survival benefit. Chemoradiotherapy has been established as the standard treatment administered post-operatively. The dose delivered during radiotherapy is 60 Gy in fractions of 2 Gy. Studies reported a significant improvement of overall and progression-free survival when RT is combined with early addition of TMZ compared to RT alone.[2] Despite this aggressive initial treatment, most patients develop recurrent disease, which can be treated with resection, systemic treatment with targeted agents or cytotoxic chemotherapy, reirradiation, or radiosurgery. Furthermore, research into novel therapies is investigating alternative TMZ regimens, convection-enhanced delivery, immunotherapy, gene therapy, antiangiogenic agents with and without cytotoxic chemotherapy and targeting of tumour growth-promoting pathways or cancer stem cell signalling pathways.[2] However, even with an optimal treatment protocol, the median survival is only 12–14 months.[1] This is because GB is characterised by a high local recurrence rate after the completion of RT. Three-dimensional (3D) conformal RT of GB is currently based on CT and MRI. Pathological changes on CT and MRI are characterised by increased water content (oedema) and leakage of the blood–brain barrier or contrast enhancement. However, both contrast-enhancement and hyperintense areas on T_2 weighted MR images are not always an accurate measure of tumour extent. Tumour cells have been detected far beyond the margins of contrast-enhancement.[3] Furthermore, in patients treated with surgery or irradiation, contrast-enhancement or increased signal intensity on T_2 weighted MR images cannot discriminate between residual tumour and post- interventional changes, such as radiation necrosis.[4] As radiation treatment is a delicate balance between tumour control and normal tissue toxicity, further treatment plan optimization can only be reached when we obtain greater knowledge of the target and a better understanding of normal tissue complications. Consequently, a major requirement to achieve better local tumour control, without increasing side-effects of RT to the adjacent normal brain, is an accurate tumour mass delineation.[5,6] As mentioned by Hoffmann et al[7] in current treatment plans the compromise between

the dose delivered to tumour and normal tissue is 'frozen', based on what is considered as the best trade-off for a specific patient population. However, additional information from functional imaging techniques, such as MR spectroscopy[8] or nuclear imaging techniques,[9,10] may have an added value for RT target volume definition because these techniques enable to visualise biologic pathways *in vivo* and may facilitate customisation of dose prescription. Because local tumour control in GB patients is still elusive in the majority of patients, there is an urgent need for alternative treatment strategies, such as the selection of an individualised dose prescription. However, to implement changes to the existing clinical standard of care, research must be conducted to develop alternative treatment strategies. Therefore, a novel approach in radiotherapy is the introduction of preclinical precision image-guided radiation research platforms. The aim of this review is to give a brief overview of the efforts that have been made in the field of radiation research using animal models of GB. Because MRI has become the reference imaging technique for treatment planning and assessment of therapeutic responses in GB patients, we will focus in this review on small animal radiotherapy combined with MRI.

Preclinical MR-guided radiation research

Treatment planning on pre-clinical radiation research platforms is mostly based on CT,[11,12] which is equivalent to human planning systems. Generally, an on-board CT system is used on these research platforms to combine accurate animal positioning and to provide electron density information necessary for individual radiation dose calculations. However, the CTs installed on these research platforms are mostly based on the cone-beam geometry, instead of conventional spiral CT used in human systems. Cone-beam CT might be hampered by low soft-tissue contrast when no antiscatter grids are used as a result of the large amount of scatter due to a high scatter-to-primary ratio on these systems.[13] Although, many investigators have shown that cone-beam CT can be extremely useful for guiding focal irradiation,[14] it remains challenging to localise soft tissue targets on cone-beam CT images. To localise soft tissue targets more efficiently, CT can be combined with other imaging modalities, where the alternative imaging technology is often used for target selection and CT is used for dose calculations and accurate beam positioning. Currently, a large number of pre-clinical non-invasive *in vivo* imaging techniques are available that have the potential to provide more detailed information compared to CT. A detailed description to facilitate the optimal use of preclinical radiation research platforms and various small animal imaging techniques can be found in.[15] This report discusses the combination of pre-clinical radiation research platforms, small animal imaging (CT, MRI, PET, SPECT, bioluminescence) systems, image registration, treatment planning, and data processing.

In this review we will focus on MRI. MRI provides vastly superior soft-tissue contrast, which makes it much easier to visualise lesion boundaries that might result in a better delineation of the target volume, helping to better irradiate the lesion and avoid surrounding tissue. An additional advantage is that MRI uses non-ionizing radio waves, unlike CT that is using ionizing radiation. The major disadvantages of MRI are the relatively long acquisition times, the high cost of an MR scanner and high operational costs. Moreover, integrating an MR-device into a pre-clinical radiation research platform is far from trivial, notwithstanding, clinical systems are currently under construction.[16–18] Because MR scans cannot be used for dose planning, as they do not provide the required electron density information, combining MR with CT data for radiation therapy planning is rapidly expanding in the clinic[19] and is the standard of care therapy in GB patients. This combined CT/MR data set contains both the information required for targeting (MR-based target volumes) and for dose calculations (CT-based electron density). However, as recommended by Verhaegen et al[15] to fully exploit the high precision of small animal image-guided radiotherapy the positioning error of the target has to be minimised and, consequently, correct registration between MR and CT is necessary to obtain accurate treatment planning. Image registration can be done manually or (semi-)automatic. Ideally, image registration should be done (semi-)automatic using, *e.g.* mutual-information-based image registration algorithms to minimise intra- and interobserver variability. In the case of brain tumours, rigid-body transformations might be sufficient for co-registration because the anatomy of the head remains relatively immobile. Despite that, MR images might be hampered by geometric distortions, mainly as a result of magnetic field inhomogeneities, and non-rigid transformations may be required to correct for possible deformations in the brain contours.[20] For accurate CT/MR registration it is recommended to use an immobilization device to minimise animal motion, to perform co-localization procedures as quickly as possible using anaesthetised animals, to provide sufficient common features by using some additional fiducial markers, such as capillary tubes, and to use an efficient co-registration algorithm.[15] When applying non-rigid transformations, it is further suggested to check that the applied corrections are realistic.

Animal models of glioblastoma

Animal models of GB can be subdivided into chemical-induced models, xenograft/allograft models and genetically engineered models (Figure 1). Chemical-induced disease model use various pharmacologically active and/or toxic compounds. For example, the F98 GB cell line was initially chemically induced by administering ethylnitrosourea to pregnant rats. The progeny of which developed brain tumours as a result of damaging DNA and inducing point mutations. These tumours were subsequently propagated *in vitro* and cloned.[21] For many years, mouse/rat and human cell lines have been used in allograft and xenograft models. Propagation and testing of GB in such animals is commonly accomplished in the subcutaneous flank location (heterotopic), however, recent years have seen increased use of orthotopic (intracranial) xenograft models.[22] Different from the heterotopic transplantation, the direct orthotopic transplantation provides a proper microenvironment and preserves the integrity of tumour-initiating cells. Xenograft/allograft model are easy to use, relatively inexpensive and reproducible. However, the main drawback of these models is that the genetics and histology of the tumours are frequently not representative of the respective human tumour.[23] Genetically engineered models are

Figure 1. Simplified overview of animal models of glioblastoma

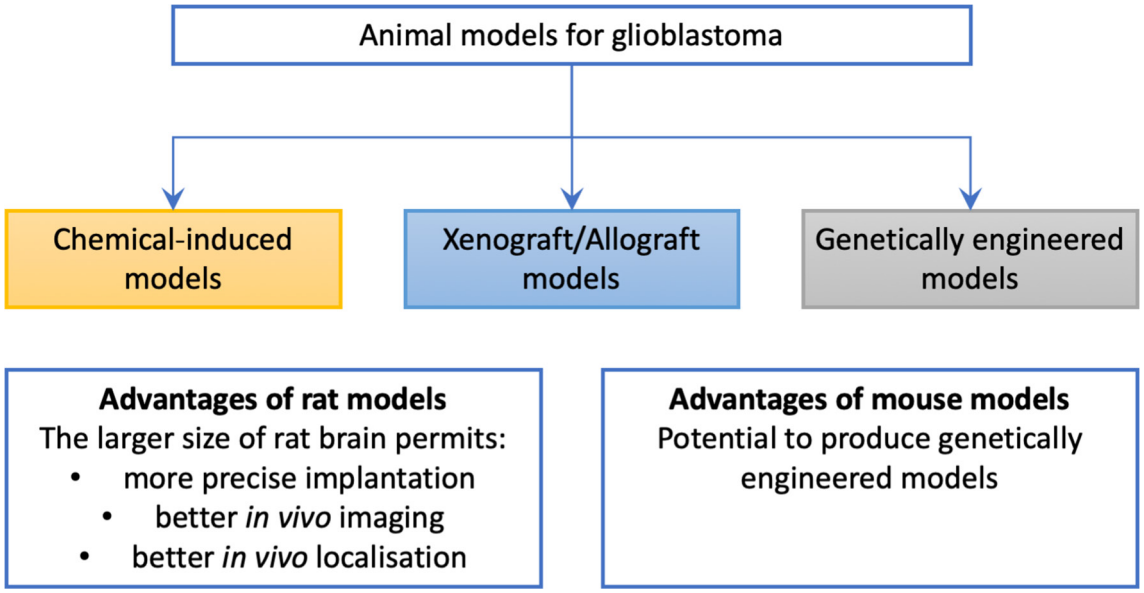

histologically and genetically more accurate models of human cancer, which involves the accumulation of genetic and epigenetic alterations that result in the loss of tumour suppressor gene function or the activation of oncogenic pathways.[22,24]

Until recently, murine models were used less frequently than rat models because the larger size of rat brain permits more precise stereotactic implantation, better *in vivo* imaging by a variety of imaging modalities and better *in vivo* localisation. By contrast, rat brain tumour models cannot be as easily genetically engineered as mouse models and rats are more expensive to purchase and maintain than mice[21] (Figure 1).

MR-guided RT in animal models of glioblastoma

Pre-clinically, only a few studies have been published that are using MR-guided treatment planning. In Figure 2, a flow chart is shown that illustrates the procedure that is applied when MRI is used to guide treatment planning.

Generally, a restraint system is used to minimise animal motion between MRI, CT and animal irradiation. This restraining device will also simplify image registration of MR and CT data. During treatment planning MRI is used to localise and determine the size of the tumour. CT information will be used to perform dose calculations and to provide anatomical landmarks to support the registration process.

In 2012, Baumann et al[25] established an image-guided radiation delivery system based on CT, MR and bioluminescent imaging in a mouse model of GB. Human-derived U251 tumour cells were transduced with a lentiviral construct containing the firefly luciferase gene and the tumour cells were implanted intracranially. T_2 weighted MR images were acquired to determine location and size of the brain tumour, to specify isocentre depth and collimator size during treatment planning, respectively. Immediately before irradiation, bioluminescent imaging was used to determine the location of maximum bioluminescent signal intensity on the animal's scalp, where a fiducial marker was attached. This fiducial marker could be visualised on the planning CT and a treatment plan was generated by combining the position of this fiducial marker with the depth of the isocentre and the collimator size, determined using MRI. The mouse's brain tumour was irradiated with one unidirectional superior-to-inferior beam. The authors confirmed that the point of maximal bioluminescent signal intensity corresponded to the centre of the tumour on MR images within ± 0.5 mm, while radiation delivery was confirmed by γH2AX staining. The authors concluded that multimodality imaging facilitated delivery of precise and reproducible cranial RT in mice that may aid future brain tumour research.

In 2014, Zhang et al[26] evaluated a hybrid image-guidance protocol, which combines on-board two-dimensional (2D) X-ray radiography with MRI, for targeted delivery of

Figure 2. MR/CT-based workflow for small animal radiation treatment.

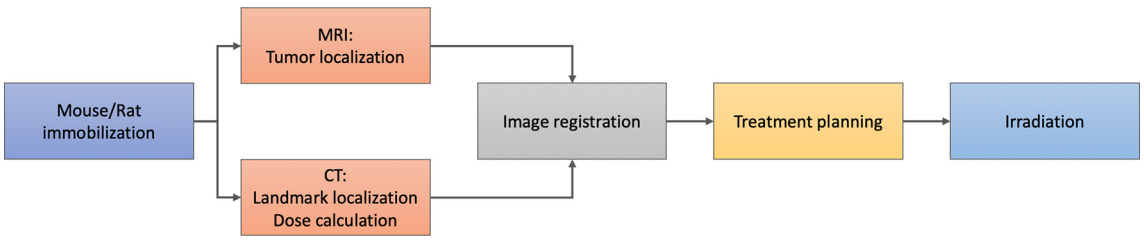

microbeam radiation therapy (MRT) in an orthotopic mouse model using U87MG human glioma tumour cells. MRT is an innovative irradiation modality, based on spatial fractionation of a high-dose X-ray beam into lattices of microbeams. U87MG human glioma tumour cells were injected intracranially into the right forebrain of nude mice with stereotactic guidance. One day before treatment, T_2 weighted MRI were acquired to delineate the tumour volumes. 2D sagittal MR projection images were generated and used for registration to sagittal X-ray projection images acquired using the on-board 2D X-ray system. A customised head-immobilizing device was fabricated by 3D printing in order to achieve accurate image registration using a rigid-body method. The number of microbeams, beam pitch, and the beam delivery locations on the tumour site, were decided based on the registered image and tumour size. Targeting accuracy was evaluated by γH2AX immunofluorescence staining. Results indicated that γH2AX foci-positive cells were clearly visible in the stained sections and corresponded to the microbeam path and spatial arrangements through the tumour and normal tissues. The authors concluded that accurate delivery of microbeams to the targeted tumour site is necessary and can be accomplished using a combined MR/X-ray image guidance procedure.

Bolcaen et al[27,28] successfully used a combined 3D CT/MR dataset for the 3D conformal irradiation of brain tumours in an orthotopic F98 GB rat model using a small animal radiation research platform. Contrast-enhanced T_1 weighted MR images were acquired to delineate the target volume during radiotherapy planning and to monitor treatment response. Rigid-body transformations in combination with an in-house developed multi-modality bed were used for image registration between MR and planning CT. To further mimic the treatment of GB in patients, rats were treated with RT and concomitant chemotherapy using TMZ. Using three non-coplanar arcs the prescribed dose could be delivered to 90% of the target volume, while minimizing the dose to normal brain tissue. Evaluation of tumour growth using contrast-enhanced T_1 weighted MR images showed that tumour volumes were stable up to 15 days post-irradiation. In contrast, exponential tumour growth was observed in a control group that received no treatment. The authors concluded that this combined CT/MR-based workflow was a major step forward in bridging the gap between preclinical and clinical radiotherapy planning, which opens the door to validate alternative treatment strategies.

In 2016, Hartmann et al[29] defined a protocol to irradiate orthotopic brain tumours in mice using a clinical linear accelerator. A clinical linear accelerator was used in order to achieve a patient-realistic situation. An in-house developed positioning applicator was used to anaesthetise and consistently position the mice during CT and irradiations. T_1 weighted MR images were acquired without this applicator. Planning CT and the MR images were manually fused to define the tumour volume using a common clinical treatment planning system (TPS). In this study, organs at risk (OARs) such as the eyes, nose and mouth were also delineated. Based on γH2AX immunohistochemically slices, a tumour conformal dose could be delivered. The authors concluded that the feasibility of precise irradiations of preclinical mouse models at nearly all centres using stereotactic clinical linear accelerators is a big advantage of their methodology. However, they also indicated possible shortcomings such as the achievable beam penumbras, which might limit the applicability for some research questions.

Finally, Gutierrez et al[30] investigated the feasibility of a MR-only based workflow for radiotherapy planning of the rat brain, that enables both accurate target delineation and accurate dose calculations using only MRI- based volumes. The image registration process between planning CT and MR images would become redundant using such an MR-only based workflow. Multiple MR sequences were used to generate synthetic CT images that could be used for dose calculations (Figure 3), because using only one MR sequence was not sufficient to separate all major tissue types (air, soft tissue, bone) in the rat head. The synthetic CT images were sufficiently similar to the segmented CT images that are routinely used for radiotherapy planning on preclinical radiation research platforms. No significant differences were observed between CT and MR based dose calculations when more complex beam configurations (multiple beams) were used in the dose plan. The authors concluded that further research is required in the thoracic or abdominal region of small animals, where more tissue classes will be required to allow for accurate dose calculations compared to the rat head. Moreover, total MRI scan time might become an issue because of animal anaesthesia and throughput, and the proposed MR-only based workflow still requires the on- board CT of the microirradiation for accurate animal positioning. For the latter, a solution should be found to ensure a common coordinate system between MR image space and microirradiator space, which is a non-trivial issue without

Figure 3. Using fuzzy c-means clustering a segmented CT image was generated using four different MR sequences: T_1W, and T_2W, UTE and ZTE. This segmented CT images can be used for dose calculations. T_1W, T_1 weighted; T_2W, T_2 weighted; UTE, ultra-short echo time; ZTE, zero echo time.

the on-board CT information. A possible solution is the use of digitally reconstructed radiographs, extracted from the acquired MR images, which may provide sufficient information for the purpose of image guidance.

MRI in animal models of glioblastoma to evaluate treatment response

MR imaging can be used not only to guide RT, but also to monitor treatment response as already mentioned in previous paragraph.[28] In the clinic, MR has successfully demonstrated that it can provide non-invasive mapping of a wide range of brain tumour characteristics (morphological and physiological) and MR has become the reference imaging technique for the assessment of therapeutic responses.[31]

Pre-clinical, these more advanced MR techniques were used by the MR research group at John Hopkins University for the assessment of response to RT in a rat model of GB.[32–34] Hong et al[34] performed longitudinal quantitative multiparametric MRI, in addition to standard T_2 weighted MR. The quantitative MR sequences included T_1 relaxometry, T_2 relaxometry, diffusion-weighted imaging (DWI), arterial spin labelling and chemical exchange-dependent saturation transfer (CEST) techniques. The primary metric derived from DWI was the apparent diffusion coefficient (ADC), which reflects the barriers and restrictions imposed by cell walls and subcellular structures on the incoherent displacement motion of water. In tumours, ADC is negatively correlated with proliferation and cellularity. Amide proton transfer (APT) was used as a specific CEST techniques that exploits the exchange between water protons and amide protons in the backbone of endogenous proteins and peptides in tissue. Tumour volume manually delineated on T_2 weighted images showed that all irradiated tumours were still growing in size 1–3 days post-irradiation. Then, these tumours remained at a size that was almost the same as the tumour size at Day 3 post-irradiation, while in a non-irradiated group all tumours grew rapidly. Multiparametric MR images revealed hyperintense T_1 and T_2 maps in the tumour region with negligible changes after RT. However, ADC values significantly increased post-irradiation, while blood flow maps (as measured by arterial spin labelling) and APT significantly decreased after radiation treatment. These results suggest that ADC, blood flow and APT signals are useful non-invasive biomarkers to predict glioma response to RT, while structural MRI are not sufficiently tissue specific to accurately measure treatment response. To further increase the accuracy of tumour localization and delineation, a semiautomatic segmentation method was evaluated to provide more reliable MR biomarkers.[32] Comparison between manual and semiautomatic analysis revealed lower intra- and interobserver variability using the semiautomatic methods, improving the accuracy of multiparametric MR. This research group also compared their multiparametric MR approach to contrast-enhanced ultrasound imaging (CEUS) and observed that several CEUS-based metrics correlated well with MR-based metrics.[33] They summarised that CEUS might be a low-cost and portable alternative to multiparametric MR for the assessment of treatment response.

The Grenoble MRI facility also determined the ability of longitudinal multiparametric MRI to distinguish the early effects of treatments during a combined chemoradiotherapy regimen in a GB rat model.[35] The combined treatment included antiangiogenic therapy using sorafenib and synchrotron MRT. Four treatment groups were included: no treatment, only antiangiogenic therapy, only MRT and combined treatment. Six complementary parameters, to characterise the physiological and cellular statuses of brain tumours, were obtained from the multiparametric MR protocol: tumour volume, ADC, blood volume fraction (BVf), vessel size index (VSI), tissue oxygen saturation (StO2) and brain- tumour barrier (BTB) permeability. Results showed that when the anti angiogenic treatment was used alone a significant decrease in tumour volume and all of the vascular-related MR parameters (BVf, VSI, StO2 and BTB permeability) was induced, when compared with the untreated group. No effect was observed on ADC. No changes of BVf, VSI or StO2 were induced by using only MRT treatment, when compared with untreated tumours. However, tumour size decreased, while ADC and BTB permeability increased. In the group that received combined therapy, an increase in ADC was observed, which would be induced by the MRT therapy. Concomitant to this ADC modification, decreases in BVf, StO2 and BTB permeability were observed, which are primarily due to the antiangiogenic treatment. However, MRT combined with antiangiogenic treatment did not induce any changes in the tumour VSI, when compared with the untreated group. These results indicate that multiparametric MR may be used in a longitudinal study to monitor the effects of different cancer therapies, where every treatment induced specific modifications upon the MR parameters. Therefore, the same group used this multiparametric MR approach to compare two radiation techniques, MRT and spatially homogeneous irradiation, to monitor treatment response in a F98 GB rat model.[36] Results showed that MRT leads to a significantly higher, earlier, and more continuous increase in tumour blood vessel permeability than spatially uniform irradiation, without affecting healthy tissue. MRT induced an increase in vascular permeability in all tumour areas with particular physiological characteristics, including those tumour areas not impacted by homogeneous irradiation, and MRT more efficiently disrupted brain tumour vessels in the most actively proliferating area of the tumour that is considered as the relevant target area for adjuvant drug delivery. The authors concluded that an adjuvant chemotherapy might be more effective when coupled with MRT than with spatially uniform irradiation fields, which are used in conventional radiation therapy.

Differentiation between tumour recurrence and radiation necrosis

Radiation treatment plays a central role in the standard of care of GB patients, however, local recurrences following therapy remain common. Like any other treatment, there are also possible side-effects associated with radiation treatment, such as delayed radiation injury, also known as radiation necrosis (RN). Obviously, a correct diagnosis is important for patient management because patients with tumour recurrence need second-line treatment, while patients with RN can continue their therapy but may require steroid administration. However, differentiation between tumour recurrence and RN presents a diagnostic

Figure 4. Glioblastoma and radiation necrosis are both heterogeneously hyperintense on T_2 weighted MR images (top). Moreover, a similar contrast enhancement pattern is observed on T_1 weighted contrast-enhanced MR images (bottom).

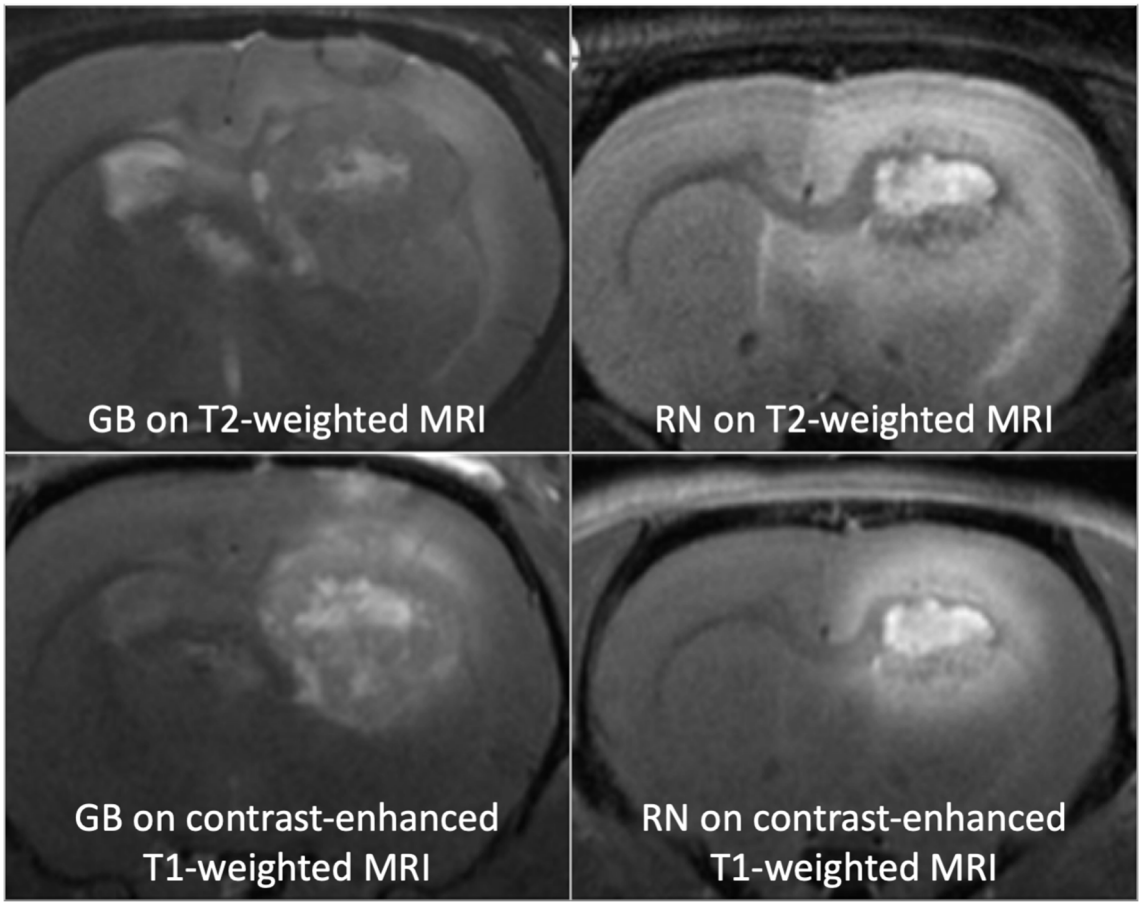

dilemma because both are usually found around the tumour bed and both entities have similar appearance on conventional MRI (Figure 4). Therefore, the differentiation between tumour recurrence and radiation necrosis has been a topic of sustained interest in laboratory animal research and often requires a combination of irradiation and advanced MRI.[37]

Until recently, reports of small-animal models of RN have been sparse, however, the arrival of small animal irradiators enabled reproducible introduction of RN in small volumes, resulting in animal models of RN in rats[37–39] and in mice.[37,40] According to Garbow et al[37] an optimised animal model of RN should incorporate several important features, such as: consistent induction of late time-to-onset necrosis following irradiation; characteristic standard MRI changes that allow clear identification of necrotic regions; tissue injury whose histology accurately matches pathological findings in brain tissue from patients with confirmed RN; progression of necrosis occurs over an experimentally appropriate period of time, thereby enabling longitudinal imaging studies to characterise the onset and development of necrosis and its response to therapeutic interventions. Using standard MRI, RN lesions are characterised as heterogeneously hyperintense on T_2 weighted MR images and contrast enhancing with surrounding oedema on T_1 weighted MR, which is similar to the appearance of GB on standard MR.[41] However, more advanced MR can provide powerful tools for differentiating RN from tumour recurrence, as illustrated in several recent studies.

Zhou et al[39] described the use of CEST-APT techniques for distinguishing tumour recurrence from radiation necrosis in rats. APT showed hyperintensities in tumours and low signals in necrotic lesions, probably associated with the absence of mobile cytosolic proteins and peptides.

Zhu et al[42] explored molecular MRI using microparticles of iron oxide (MPIO) targeted to ICAM-1. ICAM1-MPIOs caused a marked negative MRI contrast effect in irradiated rat brains, compared to rat brains that were not irradiated, probably due to the upregulated ICAM1 expression in the neuroinflammatory process in RN.

A study of the group of Garbow et al[37,43] suggested that RN and GB exhibit different DWI features in a mouse models of glioma and radiation injury. Results showed that ADC was decreased in tumours, while apparent diffusion increased in RN. The same group investigated that MR-measured tissue oxygenation changes can differentiate radiation-induced lesions from brain tumours.[37,44] MR quantification was done by evaluating the effects of the breathing gas composition on the longitudinal relaxation rate (R1). R1 data were collected during alternate free

breathing of pure oxygen, a hypoxic gas mixture (12.5% O2), and carbogen (95% O2). In each animal, three R1 data sets were randomly collected for each of the three breathing gas compositions and R1 data were collected 20 min after the start of free breathing of each gas composition to allow tissue oxygen levels to equilibrate. The authors showed that the longitudinal relaxation rate was linearly dependent upon tissue oxygenation and that radiation necrosis and tumour in mouse models can be distinguished using oxygen-driven changes in R1. Breathing gas modulation experiments applied in mice models of radiation necrosis and glioma indicated significantly larger R1 differences between the breathing gas conditions in mice with RN, compared to tumour-bearing mice.

Recently, Bolcaen et al[45] explored the use of dynamic contrast-enhanced (DCE) MRI in rats to discriminate tumour from necrosis. Time series obtained from the DCE-MRI data were used to quantify washin rate, washout rate, time-to-peak and maximum intensity. In addition, kinetic parameters were estimated using the extended Tofts model,[46,47] that has become a standard for the analysis of dynamic contrast-enhanced MRI. Significantly higher washin and washout rates were observed in GB in comparison to RN. In addition, a significantly lower time-to-peak was observed in GB compared to RN. Receiver operating characteristic (ROC) analysis was performed on these parameters and threshold values could be determined to discriminate GB from RN.

In the above studies, naïve animal models were used to create either a tumour model (that lack RN) or a model for radiation induced brain injury (that lack a tumour). Because the presence of a tumour might exacerbates radiation-induced damage in peritumoral/normal brain tissue,[48] Zawaski et al[49] investigated the effect of brain tumour presence during radiation, which corresponds more closely to the patient situation. Three groups of rats were used, a control group, a group that only received RT and a group with complete tumour regression after RT. MR spectroscopy (MRS) was performed in combination with transcriptomic analysis. Results indicated that tumour presence during radiation may affect the functional transcriptomics landscape and neurotransmitter levels at the tumour implantation site and normal tissue. MRS showed that taurine, an inhibitory neurotransmitter, was significantly lower in irradiated brains that had previously harboured a tumour, compared to the control and the group that only received RT. Taurine is a non-essential amino acid that has the ability to cross the blood–brain barrier or be synthesised within the brain by astrocytes from cysteine.[50] In the brain, taurine is involved in brain development, calcium homeostasis, osmoregulation and neurotransmission. It has been suggested that taurine may play an important role in inflammation associated with oxidative stress.[51]

Conclusions, recommendations and future perspectives

Because local tumour control in GB patients is still elusive in the majority of patients, there is an urgent need for alternative treatment strategies. With the advent of pre-clinical precision image-guided radiators, current treatment strategies might be improved by introducing new methods that can be developed to guide RT or by evaluating treatments effects more precisely. In this review, we focused on the current status of combining MRI with small animal RT using animal models of GB. Three main areas of research were found. First, MR-guided small animal RT to improve tumour localization and delineation by using the superior soft-tissue contrast properties of MR compared to CT. Second, better understanding the response to treatment by using more advanced (multiparametric) MR techniques. Finally, the discrimination between tumour recurrence and radiation necrosis remains a topic of sustained interest in laboratory animal research.

When MRI is used to guide radiation treatment it is important that MR images and planning CT are accurately co-registered. The use of a multimodality bed, some additional fiducial makers and a workflow where co-localisation procedures are performed with minimal delay can greatly simplify this process. To obtain an accurate co-registration it is further recommended to apply an automatic image registration algorithm. Although, for the head region rigid-body transformation are sufficient, non-rigid transformation might be more accurate as a result of geometric distortions of the acquired MR images.

Finally, tumour volume delineation for RT planning in GB is currently based on anatomical imaging techniques (CT/MR). It is important to mention that these structural imaging techniques cannot identify the most aggressive and/or radiation resistant parts within the tumour, which are probably responsible for treatment failure and tumour recurrence. Moreover, currently the tumour volume is being irradiated with a homogeneous dose because it is assumed that the tumour consists of tumour cells that share similar behavioural characteristics, and are therefore equally malignant and/or radiation resistant or sensitive. However, we know that tumours are very heterogeneous and using more advanced MR techniques or functional imaging techniques, such as positron emission tomography (PET), it is possible to visualise the most malignant and/or radiation resistant tumour parts. Dose painting strategies based on this functional information can be investigated preclinically before translation to the clinic. The rationale is that a non-uniform dose distribution with a higher dose to the most active and/or radiation resistant tumour regions while keeping the total tumour dose constant could improve local tumour control without adding toxicity to the adjacent brain.

REFERENCES

1. Ahmed R, Oborski MJ, Hwang M, Lieberman FS, Mountz JM. Malignant gliomas: current perspectives in diagnosis, treatment, and early response assessment using advanced quantitative imaging methods. *Cancer Manag Res* 2014; **6**: 149–70.

2. Anton K, Baehring JM, Mayer T. Glioblastoma multiforme: Overview of current treatment and future perspectives. *Hematol Oncol Clin North Am* 2012; **26**: 825–53.
3. Grosu A-L, Feldmann HJ, Dick S, Dzewas B, Nieder C, Gumprecht H, et al. Implications of IMT-SPECT for postoperative radiotherapy planning in patients with gliomas. *Int J Rad Onc *Biol* Phy* 2002; **54**: 842–54. doi: https://doi.org/10.1016/S0360-3016(02)02984-X
4. Siu A, Wind JJ, Iorgulescu JB, Chan TA, Yamada Y, Sherman JH. Radiation necrosis following treatment of high grade glioma--a review of the literature and current understanding. *Acta Neurochir* 2012; **154**: 191–201. doi: https://doi.org/10.1007/s00701-011-1228-6
5. Grosu A-L, Weber W, Feldmann HJ, Wuttke B, Bartenstein P, Gross MW, et al. First experience with I-123-alpha-methyl-tyrosine spect in the 3-D radiation treatment planning of brain gliomas. *Int J Rad Onc *Biol* Phy* 2000; **47**: 517–26. doi: https://doi.org/10.1016/S0360-3016(00)00423-5
6. Grosu AL, Weber WA. PET for radiation treatment planning of brain tumours. *Radiother Oncol* 2010; **96**: 325–7. doi: https://doi.org/10.1016/j.radonc.2010.08.001
7. Hoffmann AL, Huizenga H, Kaanders JH. Employing the therapeutic operating characteristic (TOC) graph for individualised dose prescription. *Radiat Oncol* 2013; **8**: 55: 55: . doi: https://doi.org/10.1186/1748-717X-8-55
8. Ken S, Vieillevigne L, Franceries X, Simon L, Supper C, Lotterie JA, et al. Integration method of 3D MR spectroscopy into treatment planning system for glioblastoma IMRT dose painting with integrated simultaneous boost. *Radiat Oncol* 2013; **8**: 1–9. doi: https://doi.org/10.1186/1748-717X-8-1
9. Li FM, Nie Q, Wang RM, Chang SM, Zhao WR, Zhu Q, et al. 11C-CHO PET in optimization of target volume delineation and treatment regimens in postoperative radiotherapy for brain gliomas. *Nucl Med Biol* 2012; **39**: 437–42. doi: https://doi.org/10.1016/j.nucmedbio.2011.10.003
10. Niyazi M, Geisler J, Siefert A, Schwarz SB, Ganswindt U, Garny S, et al. FET-PET for malignant glioma treatment planning. *Radiother Oncol* 2011; **99**: 44–8. doi: https://doi.org/10.1016/j.radonc.2011.03.001
11. Verhaegen F, Granton P, Tryggestad E. Small animal radiotherapy research platforms. *Phys Med Biol* 2011; **56**: R55–R83. doi: https://doi.org/10.1088/0031-9155/56/12/R01
12. Butterworth KT, Prise KM, Verhaegen F. Small animal image-guided radiotherapy: status, considerations and potential for translational impact. *Br J Radiol* 2015; **88**: 20140634–6. doi: https://doi.org/10.1259/bjr.20140634
13. Siewerdsen JH, Moseley DJ, Bakhtiar B, Richard S, Jaffray DA. The influence of antiscatter grids on soft-tissue detectability in cone-beam computed tomography with flat-panel detectors. *Med Phys* 2004; **31**: 3506–20. doi: https://doi.org/10.1118/1.1819789
14. Verhaegen F, van Hoof S, Granton PV, Trani D. A review of treatment planning for precision image-guided photon beam pre-clinical animal radiation studies. *Zeitschrift für Medizinische Physik* 2014; **24**: 323–34. doi: https://doi.org/10.1016/j.zemedi.2014.02.004
15. Verhaegen F, Dubois L, Gianolini S, Hill MA, Karger CP, Lauber K, et al. ESTRO ACROP:Technology for precision small animal radiotherapy research: Optimal use and challenges. *Radiother Oncol* 2017; . . The Authors.
16. Wooten HO, Rodriguez V, Green O, Kashani R, Santanam L, Tanderup K, et al. Benchmark IMRT evaluation of a Co-60 MRI-guided radiation therapy system. *Radiother Oncol* 2015; **114**: 402–5. doi: https://doi.org/10.1016/j.radonc.2015.01.015
17. Wooten HO, Green O, Yang M, DeWees T, Kashani R, Olsen J, et al. Quality of intensity modulated radiation therapy treatment plans using a 60 Co magnetic resonance image guidance radiation therapy system. *Int J Rad Onc *Biol* Phy* 2015; **92**: 771–8. doi: https://doi.org/10.1016/j.ijrobp.2015.02.057
18. Lagendijk JJ, Raaymakers BW, Van den Berg CA, Moerland MA, Philippens ME, van Vulpen M. MR guidance in radiotherapy. *Phys Med Biol* 2014; **59**: R349–R369. doi: https://doi.org/10.1088/0031-9155/59/21/R349
19. Schmidt MA, Payne GS. Radiotherapy planning using MRI. *Phys Med Biol* 2015; **60**: R323–R361. doi: https://doi.org/10.1088/0031-9155/60/22/R323
20. Pappas EP, Dellios D, Seimenis I, Moutsatsos A, Georgiou E, Karaiskos P. Review and comparison of geometric distortion correction schemes in MR images used in stereotactic radiosurgery applications. *J Phy: Conf Ser* 2017; **931**: 012031. doi: https://doi.org/10.1088/1742-6596/931/1/012031
21. Barth RF, Kaur B. Rat brain tumor models in experimental neuro-oncology: the C6, 9L, T9, RG2, F98, BT4C, RT-2 and CNS-1 gliomas. *J Neurooncol* 2009; **94**: 299–312. doi: https://doi.org/10.1007/s11060-009-9875-7
22. Miyai M, Tomita H, Soeda A, Yano H, Iwama T, Hara A. Current trends in mouse models of glioblastoma. *J Neurooncol* 2017; **135**: 423–32. doi: https://doi.org/10.1007/s11060-017-2626-2
23. Becher OJ, Holland EC. Genetically engineered models have advantages over xenografts for preclinical studies. *Cancer Res* 2006; **66**: 3355–9. doi: https://doi.org/10.1158/0008-5472.CAN-05-3827
24. Agnihotri S, Burrell KE, Wolf A, Jalali S, Hawkins C, Rutka JT, et al. Glioblastoma, a brief review of history, molecular genetics, animal models and novel therapeutic strategies. *Arch Immunol Ther Exp* 2013; **61**: 25–41. doi: https://doi.org/10.1007/s00005-012-0203-0
25. Baumann BC, Benci JL, Santoiemma PP, Chandrasekaran S, Hollander AB, Kao GD, et al. An integrated method for reproducible and accurate image-guided stereotactic cranial irradiation of brain tumors using the small animal radiation research platform. *Transl Oncol* 2012; **5**: 230–7. doi: https://doi.org/10.1593/tlo.12136
26. Zhang L, Yuan H, Burk LM, Inscoe CR, Hadsell MJ, Chtcheprov P, et al. Image-guided microbeam irradiation to brain tumour bearing mice using a carbon nanotube x-ray source array. *Phys Med Biol* 2014; **59**: 1283–303. doi: https://doi.org/10.1088/0031-9155/59/5/1283
27. Bolcaen J, Descamps B, Boterberg T, Vanhove C, Goethals I. PET and MRI Guided Irradiation of a Glioblastoma Rat Model Using a Micro-irradiator. *J Vis Exp* 2017; **130**: 1–10.
28. Bolcaen J, Descamps B, Deblaere K, Boterberg T, Hallaert G, Van den Broecke C, et al. MRI-guided 3D conformal arc micro-irradiation of a F98 glioblastoma rat model using the Small Animal Radiation Research Platform (SARRP. *J Neurooncol* 2014; **120**: 257–66. doi: https://doi.org/10.1007/s11060-014-1552-9
29. Hartmann J, Wölfelschneider J, Stache C, Buslei R, Derer A, Schwarz M. Neuartige Bestrahlungsmethode für stereotaktische Hochpräzisionsbestrahlung vonMaushirnen. *Strahlentherapie und Onkol* 2016; **192**: 806–14.
30. Gutierrez S, Descamps B, Vanhove C. MRI-Only Based Radiotherapy Treatment Planning for the Rat Brain on a Small Animal Radiation Research Platform (SARRP. *Plos One* . 2015; **10**: e0143821. doi: https://doi.org/10.1371/journal.pone.0143821
31. Preusser M, de Ribaupierre S, Wöhrer A, Erridge SC, Hegi M, Weller M, et al. Current concepts and management of glioblastoma.

Ann Neurol 2011; **70**: 9–21. doi: https://doi.org/10.1002/ana.22425

32. Yu Y, Lee DH, Peng SL, Zhang K, Zhang Y, Jiang S, et al. Assessment of Glioma Response to Radiotherapy Using Multiple MRI Biomarkers with Manual and Semiautomated Segmentation Algorithms. *J Neuroimaging* 2016; **26**: 626–34. doi: https://doi.org/10.1111/jon.12354
33. Yang C, Lee DH, Mangraviti A, Su L, Zhang K, Zhang Y, et al. Quantitative correlational study of microbubble-enhanced ultrasound imaging and magnetic resonance imaging of glioma and early response to radiotherapy in a rat model. *Med Phys* 2015; **42**: 4762–72. doi: https://doi.org/10.1118/1.4926550
34. Hong X, Liu L, Wang M, Ding K, Fan Y, Ma B, et al. Quantitative multiparametric MRI assessment of glioma response to radiotherapy in a rat model. *Neuro Oncol* 2014; **16**: 856–67. doi: https://doi.org/10.1093/neuonc/not245
35. Lemasson B, Bouchet A, Maisin C, Christen T, Le Duc G, Rémy C, et al. Multiparametric MRI as an early biomarker of individual therapy effects during concomitant treatment of brain tumours. *NMR in Biomedicine* 2015; **28**: 1163–73. doi: https://doi.org/10.1002/nbm.3357
36. Bouchet A, Potez M, Coquery N, Rome C, Lemasson B, Bräuer-Krisch E, et al. Permeability of brain tumor vessels induced by uniform or spatially microfractionated synchrotron radiation therapies. *Int J Rad Onc *Biol* Phy* 2017; **98**: 1174–82. doi: https://doi.org/10.1016/j.ijrobp.2017.03.025
37. Garbow JR, Tsien CI, Beeman SC. Preclinical MRI: Studies of the irradiated brain. *J Magn Reson* 2018; **292**: 73–81. doi: https://doi.org/10.1016/j.jmr.2018.03.011
38. Kumar S, Arbab AS, Jain R, Kim J, deCarvalho AC, Shankar A, et al. Development of a novel animal model to differentiate radiation necrosis from tumor recurrence. *J Neurooncol* 2012; **108**: 411–20. doi: https://doi.org/10.1007/s11060-012-0846-z
39. Zhou J, Tryggestad E, Wen Z, Lal B, Zhou T, Grossman R, et al. Differentiation between glioma and radiation necrosis using molecular magnetic resonance imaging of endogenous proteins and peptides. *Nat Med* 2011; **17**: 130–4. doi: https://doi.org/10.1038/nm.2268
40. Jost SC, Hope A, Kiehl E, Perry A, Travers S, Garbow JR. A novel murine model for localized radiation necrosis and its characterization using advanced magnetic resonance imaging. *Int J Rad Onc *Biol* Phy* 2009; **75**: 527–33. doi: https://doi.org/10.1016/j.ijrobp.2009.06.007
41. Alexiou GA, Tsiouris S, Kyritsis AP, Voulgaris S, Argyropoulou MI, Fotopoulos AD. Glioma recurrence versus radiation necrosis: accuracy of current imaging modalities. *J Neurooncol* 2009; **95**: 1–11. doi: https://doi.org/10.1007/s11060-009-9897-1
42. Zhu Y, Ling Y, Zhong J, Liu X, Wei K, Huang S. Magnetic resonance imaging of radiation-induced brain injury using targeted microparticles of iron oxide. *Acta Radiol* 2012; **53**: 812–9. doi: https://doi.org/10.1258/ar.2012.120040
43. Perez-Torres CJ, Engelbach JA, Cates J, Thotala D, Yuan L, Schmidt RE, et al. Toward distinguishing recurrent tumor from radiation necrosis: DWI and MTC in A gamma Knife–Irradiated mouse glioma model. *Int J Rad Onc *Biol* Phy* 2014; **90**: 446–53. doi: https://doi.org/10.1016/j.ijrobp.2014.06.015
44. Beeman SC, Shui YB, Perez-Torres CJ, Engelbach JA, Ackerman JJ, Garbow JR. O2 -sensitive MRI distinguishes brain tumor versus radiation necrosis in murine models. *Magn Reson Med* 2016; **75**: 2442–7. doi: https://doi.org/10.1002/mrm.25821
45. Bolcaen J, Descamps B, Acou M, Deblaere K, den Broecke CV, Boterberg T, et al. In Vivo DCE-MRI for the Discrimination Between Glioblastoma and Radiation Necrosis in Rats. *Mol Imaging Biol* 2017; **19**: 857–66. doi: https://doi.org/10.1007/s11307-017-1071-0
46. Sourbron SP, Buckley DL. On the scope and interpretation of the Tofts models for DCE-MRI. *Magn Reson Med* 2011; **66**: 735–45. doi: https://doi.org/10.1002/mrm.22861
47. Tofts PS, Brix G, Buckley DL, Evelhoch JL, Henderson E, Knopp MV, et al. Estimating kinetic parameters from dynamic contrast-enhanced T(1)-weighted MRI of a diffusable tracer: standardized quantities and symbols. *J Magn Reson Imaging* 1999; **10**: 223–32. doi: https://doi.org/10.1002/(SICI)1522-2586(199909)10:3<223::AID-JMRI2>3.0.CO;2-S
48. Zawaski JA, Gaber MW, Sabek OM, Wilson CM, Duntsch CD, Merchant TE. Effects of irradiation on brain vasculature using an in situ tumor model. *Int J Rad Onc *Biol* Phy* 2012; **82**: 1075–82. doi: https://doi.org/10.1016/j.ijrobp.2011.06.1984
49. Zawaski JA, Sabek OM, Voicu H, Eastwood Leung H-C, Gaber MW. Effect of brain tumor presence during radiation on tissue toxicity: Transcriptomic and metabolic changes. *Int J Rad Onc *Biol* Phy* 2017; **99**: 983–93. doi: https://doi.org/10.1016/j.ijrobp.2017.07.010
50. Pow DV, Sullivan R, Reye P, Hermanussen S. Localization of taurine transporters, taurine, and (3)H taurine accumulation in the rat retina, pituitary, and brain. *Glia* 2002; **37**: 153–68. doi: https://doi.org/10.1002/glia.10026
51. Marcinkiewicz J, Kontny E. Taurine and inflammatory diseases. *Amino Acids* 2014; **46**: 7–20. doi: https://doi.org/10.1007/s00726-012-1361-4